International Journal of Pharmaceutics 547 (2018) 438–449

Contents lists available at ScienceDirect

International Journal of Pharmaceutics

journal homepage: www.elsevier.com/locate/ijpharm

Effect of photo-degradation on the structure, stability, aggregation, and function of an IgG1 monoclonal antibody

Dinen D. Shah[a], Jingming Zhang[c], Haripada Maity[b,*], Krishna M.G. Mallela[a,*]

[a] Department of Pharmaceutical Sciences & Center for Pharmaceutical Biotechnology, Skaggs School of Pharmacy and Pharmaceutical Sciences, University of Colorado Anschutz Medical Campus, Aurora, CO 80045, United States
[b] Biophysical Characterization, Formulation Development, Eli Lilly and Company, Branchburg, NJ 08876, United States
[c] Bioanalytical Sciences, Eli Lilly and Company, Branchburg, NJ 08876, United States

ARTICLE INFO

Keywords:
Photo-oxidation
Structure
Stability
Aggregation
Function
Excipients
mAb

ABSTRACT

Photostability testing of therapeutic proteins is a critical requirement in the development of biologics. Upon exposure to light, pharmaceutical proteins may undergo a change in structure, stability, and functional properties that could have a potential impact on safety and efficacy. In this work, we studied how exposure to light, according to ICH guidelines, leads to photo-oxidation of a therapeutic IgG1 mAb. We also tested the ability of five different excipients to prevent such oxidation. In samples that were exposed to light, we found that the C_H2 domain was considerably destabilized but there were no major changes in the overall structure of the protein. Aggregation of the protein was observed because of light exposure. Mass spectrometry identified that light exposure oxidizes two key methionine residues in the Fc region of the protein. In terms of function, a loss in binding to the neonatal Fc receptor, decreased antibody-dependent cell-mediated cytotoxicity and cell proliferation activities of the protein were seen. Combined analysis of the photo-oxidation effects on the structure, stability, aggregation, and function of the mAb has identified the underlying unifying mechanism. Among the sugars and amino acids tested, methionine was the most effective in protecting mAb against photo-oxidation.

1. Introduction

Among the over 70 US FDA approved therapeutic protein products since 2011, more than half belong to the class of monoclonal antibodies (FDA, 2017; Lagasse et al., 2017). Like all proteins, they are vulnerable to light-induced degradation which can adversely affect product safety and quality (Kerwin and Remmele, 2007; Li et al., 1995). Therapeutic proteins may be exposed to both visible and UV light from manufacturing through use by the patient. Exposure to light can come from normal laboratory and GMP processing protocols (Sreedhara et al., 2016). Additional exposure can come from purification and during dilution and administration via IV bags. Visual inspection of products exposes antibody formulations to a more intense light exposure than room light (Rathore et al., 2010). Light exposure leads to oxidation, which may eventually result in protein aggregation and subsequent loss of safety and efficacy of therapeutic proteins (Torosantucci et al., 2014). Because of these detrimental effects on product quality, regulatory agencies require photostability studies when assessing protein drug products for marketing authorization.

Current International Council for Harmonization of Technical Requirements for Pharmaceuticals for Human Use (ICH) guidelines (Q1B) recommend testing for photostability of protein formulations using both visible and UV light at stipulated intensity (Nowak et al., 2017; Q1B, 1997). These guidelines can help predict the degradation pathways for proteins which can in turn lead to developing preventive strategies to mitigate the issue. Additionally, light exposure can lead to degradation of formulation excipients such as polysorbates which can give rise to reactive oxygen species and thereby lead to oxidation of proteins (Ha et al., 2002; Kerwin, 2008; Kishore et al., 2011a; Lam et al., 1997). Light-induced degradation is not limited to liquid products, it can also occur in solid lyophilized products (Miller et al., 2003). All biologic products carry an inherent risk of viral presence and several steps are required to inactivate and clear the viral presence from the finished drug product (Cipriano et al., 2012). Exposing to UV-C light is one such method used for this viral inactivation process, during which photo-oxidation can occur (Lorenz et al., 2009). Additionally,

Abbreviations: mAb, monoclonal antibody; Fc, fragment crystallizable; FcRn, neonatal Fc receptor; ADCC, antibody dependent cell-mediated cytotoxicity; ROS, reactive oxygen species; ICH, International Council for Harmonization of Technical Requirements for Pharmaceuticals for Human Use

* Corresponding author at: Department of Pharmaceutical Sciences, University of Colorado Anschutz Medical Campus, 12850 E Montview Blvd, MS C238, Aurora, CO 80045, United States (K.M.G. Mallela).
E-mail addresses: haripada.maity@yahoo.com (H. Maity), krishna.mallela@ucdenver.edu (K.M.G. Mallela).

https://doi.org/10.1016/j.ijpharm.2018.06.007
Received 25 March 2018; Received in revised form 31 May 2018; Accepted 4 June 2018
Available online 05 June 2018
0378-5173/

photo-oxidation can depend on the headspace oxygen in filled drug product vials (Cleland et al., 1993; Qi et al., 2009; Roy et al., 2009). Buffers containing histidine can degrade due to light exposure (Zbacnik et al., 2017). With the advent of antibody-drug conjugates (ADCs) as another modality for biologics, this issue becomes even more critical to study as most of the anti-cancer drugs that are currently attached to the antibodies have aromatic groups and many of them are photosensitive (Cockrell et al., 2015). Just an hour of exposure to ambient light has been shown to induce aggregation of an ADC (Cockrell et al., 2015).

The primary targets of photodegradation of proteins in the near-UV region are the aromatic amino acids and cysteine. The absorbed light leads to excitation of electrons to higher energy singlet state. This could be followed by diverse processes that include fluorescence, phosphorescence, generation of singlet oxygen, or photoionization (Bommana et al., 2018; Cleland et al., 1993; Kerwin and Remmele, 2007). Photodegradation generated reactive oxygen species (ROS) can lead to subsequent oxidation of amino acid residues. Alternatively, excipients like polysorbates may undergo photodegradation and generate hydroxyl radicals and singlet oxygen that can cause oxidation of amino acid residues (Lam et al., 1997). Proteins do not absorb visible light but tryptophan degradation products like kynurenine, N-formyl kynurenine and hydroxyl tryptophan can absorb in the visible region and act as photosensitizers (Du et al., 2018; Kerwin and Remmele, 2007). Therefore, it is important to understand the effect of both UV and visible light on the photo degradation profile of proteins.

In this study, we examined the effect of photo-oxidation on the structure, stability, aggregation, and function for a specific IgG1 mAb (Fig. 1A), in particular mAb8 from Eli Lilly and Company. We tested the protective nature of various excipients that include amino acids methionine, tryptophan and arginine, and sugars such as sucrose and trehalose. Free methionine is a known radical scavenger/sacrificial agent that can help prevent oxidation (Knepp et al., 1996; Lam et al., 1997). The photo degradation of tryptophan is known to generate reactive oxygen species (Li et al., 2014b; Sreedhara et al., 2013), and it was used here as a positive control to determine the effect of accelerated photo degradation on mAb8. Arginine is hypothesized to protect proteins against aggregation by weakly interacting with the aromatic residues in proteins and by weak electrostatic interactions with proteins (Arakawa et al., 2007a,b; Maity et al., 2009; Sudrik et al., 2017). The disaccharides sucrose and trehalose have been known to increase the thermodynamic stability of proteins by the phenomenon of preferential exclusion (Chi et al., 2003; DePaz et al., 2000; Kendrick et al., 1997; Timasheff, 2002). To our knowledge, this is the first detailed study that seeks to understand the effects of photo-oxidation on a mAb from different perspectives of structure and function, and examines whether there exists an unifying mechanism that can interpret these changes with the site and extent of photo-oxidation.

2. Materials and methods

2.1. Materials

IgG1 monoclonal antibody (mAb8) was provided by Eli Lilly and Company. All experiments were done in formulation buffer, containing citrate, NaCl, mannitol, glycine, and polysorbate 80, pH 6, unless otherwise mentioned. Methionine, tryptophan, arginine, sucrose and trehalose were purchased from Sigma-Aldrich. PD-10 columns were purchased from GE healthcare (GE Healthcare, catalog # 17085101).

2.2. Reaction and quenching

Photodegradation of mAb8 was done as per ICH guidelines (Q1B, 1997) on the Caron 6510 Series Photostability chamber (Expose 1 cycle-1.2 million lux hours of visible light (400–700 nm), 200 W-h/m^2 of UVA light (320–400 nm)). The dark control and the light exposed samples were both stored in the photostability chamber after crimping the 15 ml glass vials with rubber stopper. mAb8 was used at a concentration of 10 mg/ml.

Met and Trp concentration were 260 mM and 19.6 mM. Arginine HCl, sucrose and trehalose dihydrate were all used at 100 mM. Concentrations for Met and Trp were chosen close to saturating conditions to test for the maximum protective and damaging effects respectively, Arg was chosen at 100 mM as it has been shown to successfully prevent protein aggregation at this concentration, and higher concentrations of Arg can sometimes lead to unfavorable interactions (Sudrik et al., 2017). After the recommended light exposure, all the samples were passed through two gel filtration PD10 columns for complete removal of any oxidant or free amino acid. No visible aggregates were seen in any of the samples. Samples were then stored at 4 °C in dark in the formulation buffer for further studies.

2.3. SDS-PAGE

SDS-PAGE was run using Tris-Glycine running buffer (25 mM Tris, 192 mM glycine, 0.1% SDS at pH-8.3). A 4–20% mini-protean TGX precast protein gel from Biorad was used. Protein was loaded into each well after treating it with 2-mercaptoethanol for 5 min and boiling the samples at 100 °C for 5 min. Samples were centrifuged for 2 min at 15,000*g* before loading.

2.4. Circular dichroism (CD) spectroscopy

Far and near-UV CD measurements were done at a protein concentration of 0.1 mg/ml with 0.1 cm pathlength cuvette, and 1 mg/ml with 1 cm pathlength cuvette (1 × 1 cm) respectively using Jasco J-810 polarimeter. Data was collected at a 0.5 nm interval with a response time of 4 s in the wavelength range of 190–250 nm for far-UV CD and 250–330 nm for near-UV CD. The bandwidth and slit widths were 2 nm and 1 mm respectively. Each spectrum was the average of four scans. The corresponding buffer spectrum was subtracted from the recorded protein spectrum, and the subtracted spectrum was then normalized using the protein concentration measured on the corresponding CD samples. For far-UV CD, all samples were buffer exchanged into phosphate buffered saline (PBS), 10 mM Na Phosphate, 150 mM NaCl, pH 7.0 before recording spectra to circumvent interference from the formulation buffer components. Near-UV CD spectra were recorded directly in the formulation buffer because none of the buffer components absorb in this wavelength region. All spectra were recorded at 25 °C.

2.5. Fluorescence spectroscopy

Fluorescence spectra were recorded using a 1 cm pathlength cuvette (1 cm × 1 cm) at a protein concentration of 0.25 mg/ml using Cary Eclipse EL07013879 fluorometer (Varian). The excitation wavelength was 295 nm, and the emission was monitored from 310 nm to 450 nm. The buffer spectrum was subtracted from the recorded protein spectrum, and the subtracted spectrum was then normalized using the protein concentration directly measured on the corresponding fluorescence sample. Each reported spectrum was the average of 4 scans and all measurements were done at 25 °C.

2.6. Differential scanning calorimetry (DSC)

Protein stability was measured using a MicroCal VP-Capillary DSC at a protein concentration of 1 mg/ml and with a scan rate of 60 °C/h in the temperature range of 20–95 °C. The solutions were pressurized at 60 psi in the capillaries during each scan. Buffer/buffer scan was subtracted from buffer/protein scan and a temperature range of the thermogram around the peak was selected. The baseline correction was performed and the thermogram was normalized for protein concentration. Midpoint of thermal denaturation (T_m) was determined as the peak maximum in DSC thermograms.

2.7. Size exclusion chromatography (SEC)

SEC analysis was performed at 25 °C using a TSK Gel G3000SW$_{XL}$ column at a flow rate of 0.3 ml per min. 2 mg/ml protein with 10 µl injection volume was loaded on SEC column. Mobile phase used was 10 mM sodium phosphate, 500 mM cesium chloride, pH 7. SEC chromatograms were recorded by monitoring absorbance at 280 nm. Cesium chloride was used to minimize non-specific interaction of the protein with the column matrix (Bruner et al., 1997).

2.8. Dynamic light scattering (DLS)

Hydrodynamic radius (R_H) was determined using Wyatt DynaPro Plate Reader at a protein concentration of 2 mg/ml in batch mode. Twenty acquisitions were collected for each measurement and each acquisition was for 3 sec. For determination of hydrodynamic radius, a default value of 1.333 at 20 °C was used for the refractive index of the protein at 589 nm.

2.9. Functional characterization

2.9.1. FcRn binding assay

20 µg/ml of FcRn was immobilized onto a CM5 flow cell. A calibration curve was created in the concentration range 39–1000 ng/ml diluted at 1:1.5 using the mAb8 product reference standard. The mAb8 samples were tested at five concentrations in the range 98.7–500 ng/ml as determined from absorbance at 280 nm. 10 mM sodium phosphate, 150 mM NaCl, 3 mM EDTA, 0.05% w/v polysorbate 20, pH 5.8 was used as the running buffer and as the sample dilution buffer. The surface was regenerated for 10 s at a flow rate of 60 ml/min using 10 mM sodium phosphate, 500 mM NaCl, 0.05% w/v polysorbate 20, pH 7.2. An assay control of 250 ng/ml mAb8 was used to ensure assay stability. The calculated concentrations of the samples were based on 4-parameter regression analysis of the product standard curve. The concentration of mAb8 in a sample was calculated from its resonance units by comparison to the resonance units of solutions containing known amounts of mAb8 standard. The binding activity was calculated from mean calculated concentration of mAb8 from five dilutions divided by the protein concentration determined from absorbance at 280 nm times 100.

2.9.2. Antibody dependent cell-mediated cytotoxicity (ADCC) assay

Target cells (human colon cancer cell line HCC827) were seeded in a 96-well plate and incubated overnight at 37 °C, 7% CO_2. After 16–21 h, cells were first incubated with serial dilutions of antibody for 1 h, and then with Jurkat-vv-NFAT-Luc cells at a fixed effector: target cell ratio of 1:5 for 3–4 h at 37 °C, 7% CO_2. Antibody and effector cell dilutions were performed in serum free assay medium. Target and effector cells as well as antibody dilutions were added in 50 µl volume each. Luciferase activity of activated effector cells was measured by incubating cells with Bright-Glo™ Luciferase substrate and reading in a microtiter plate reader to obtain a relative luminescent signal (RLU). Activation of effector cells, and hence antibody activity is directly proportional to the luminescent signal from luciferase activity. Data was analyzed by Softmax Pro 5.4.4 software to generate dose response curve. The relative ADCC activity was calculated using the formula ((D − A)/C) × 100.

2.9.3. Target protein receptor binding assay

Binding of mAb8 to target protein receptor was measured using Biacore C. The receptor was immobilized onto a CM5 flow cell and a calibration curve was created with concentrations in the range 78–2000 ng/mL using the product reference standard. The samples were tested at five concentrations ranging from 117 ng/mL to 889 ng/mL based on the protein concentration determined from absorbance at 280 nm. The calculated concentrations of the samples were based on 4-parameter regression analysis of the product standard. The concentration of mAb8 in a sample was calculated from its resonance units by comparison to the resonance units of solutions containing known amounts of the standard. The potency values, reported as % activity, were calculated from mean calculated concentration of mAb8 from five dilutions divided by the protein concentration determined from absorbance at 280 nm times 100.

2.9.4. Cell proliferation assay

The ability of mAb8 to inhibit the growth of DiFi cells (rectal carcinoma cell line) in culture was performed by measuring ATP production which reflects cell number. In this assay, a 96-well plate was seeded with DiFi cells (10,000 cells/well). Known concentrations of mAb8 reference standard and the light exposed samples ranging from 0.13 nM to 5 nM were added to each well. The potency of mAb8 was measured by comparing the growth of the DiFi cells without and with the addition of mAb8. After incubation for 96 h at 37 °C/7% CO_2, cell viability was measured based on the amount of ATP produced by the metabolically active cells in the culture. The produced ATP was measured by the conversion of luciferin to oxyluciferin by luciferase enzyme. The luminescence generated during the process was measured using a plate reader with luminescence detection. The luminescence is proportional to the amount of ATP present, which in turn is proportional to the number of viable cells. Higher luminescence is indicative of a higher number of viable cells and lower inhibition of the growth of the DiFi cells. The data was analyzed by using the equation,

$$\% \text{ Biological Activity} = 100 \times (IC_{50} \text{ of mAb8 reference standard} / IC_{50} \text{ of unknown sample})$$

2.10. Peptide mapping by LC-MS

About 100 µg of mAb8 samples were dried completely using speedvac before they were denatured and reduced by 50 mM DTT (Thermofisher) in 7.2 M guanidinium chloride (GdmCl), 100 mM Tris, pH 7.5 buffer. The reduced samples were alkylated with 125 mM iodoacetamide dissolved in 100 mM Tris, pH 7.5. The reduced and alkylated samples were dialyzed in 50 mM Tris, pH 7.5 buffer using a 96-well micro-dialysis plate (Thermofisher) for 1.5–2 h with two diluent changes. The digestion was done with 1:20 trypsin (Promega) to protein ratio at 37 °C for 3 hrs. The samples were analyzed by LC-MS (1200 Agilent; LTQ Orbitrap XL, Thermo) using AdvancedBio peptide column (2.1 × 150 mm, 2.7 µM) from Agilent with a mobile phase A of 0.1% trifluoroacetic acid in H_2O and B of 0.085% trifluoroacetic acid in acetonitrile. The HPLC gradient was 0% B to 40% B in 95 min with a flow rate of 0.2 ml/min and 50 °C column temperature. Modifications were identified from the MS and MS/MS data, and relative percentages of modifications were calculated using extracted ion chromatograms (XIC) of integrated peak areas of corresponding modified and unmodified peptides using Protein Metrics software.

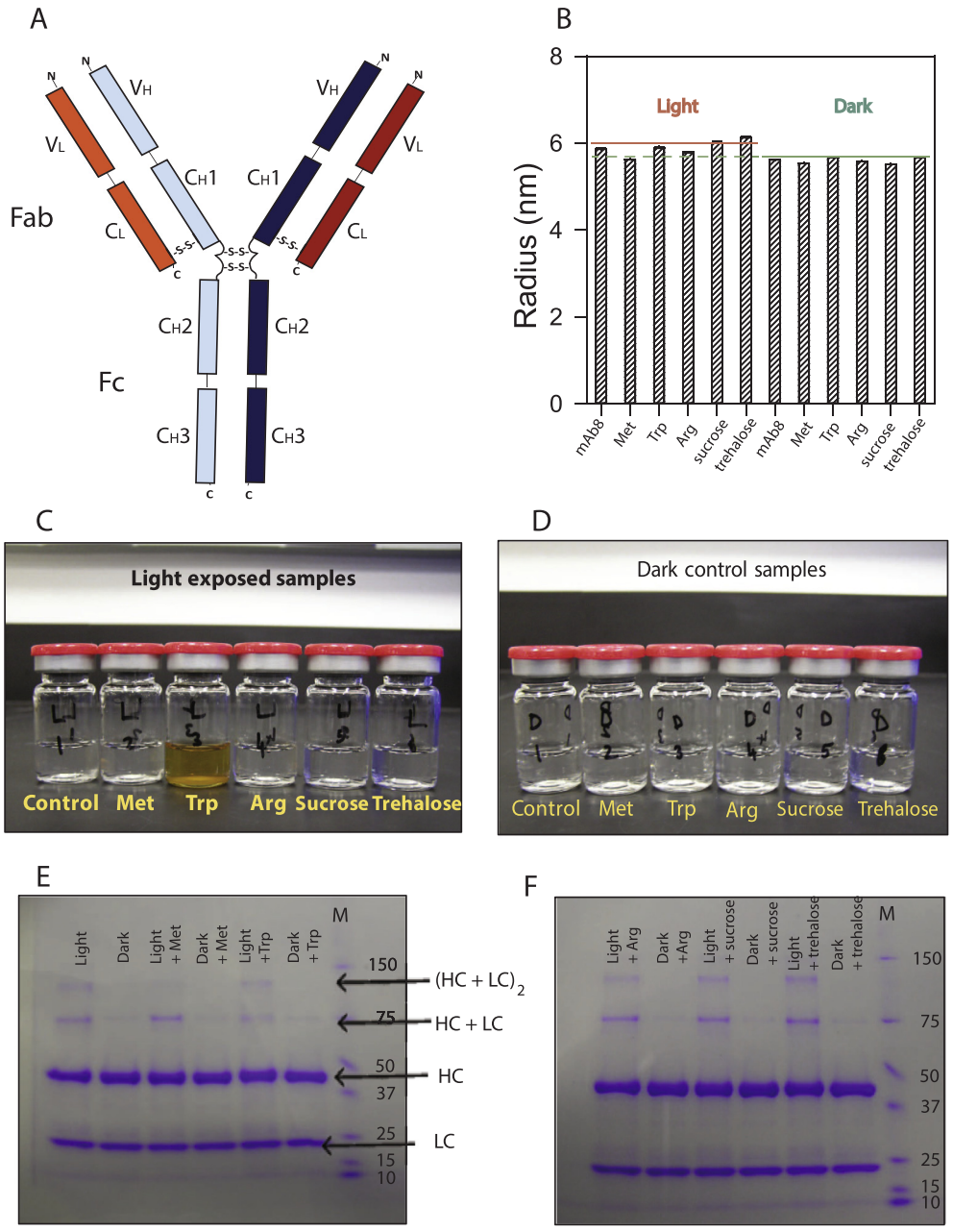

Fig. 1. (A) Structure of an IgG1 mAb composed of 2 heavy (subscript H; blue colored) and 2 light (subscript L; red colored) chains, with each chain having variable (V) and constant (C) domains. Each heavy chain consists of 3 constant domains (C_H1, C_H2, and C_H3) and 1 variable domain (V_H), whereas each light chain consists of 1 constant domain (C_L) and 1 variable domain (V_L). Figure also shows the N- and C-termini of the light and heavy chains. (B) Hydrodynamic radii of mAb8 samples determined from dynamic light scattering (DLS) measurements. (C) Light exposed samples after completion of the exposure cycle as per ICH guidelines in the photostability chamber. (D) Dark control samples after keeping in the photostability chamber for the same amount of time as those of samples in panel C. (E & F) SDS-PAGE of different samples run under reducing conditions. HC and LC refer to heavy and light chains, respectively.

3. Results

3.1. Photo-oxidation of mAb8

Following the ICH guidelines Q1B (2) (Q1B, 1997), mAb8 samples in formulation buffer were exposed for 1.2 million lux hours of visible light (400–700 nm), 200 W-h/m^2 of UV light (320–400 nm with maximum energy emission between 350 and 370 nm) without and with potential protective excipients. The light exposed samples were stored in clear glass vials and the dark control samples were covered with aluminum foil and placed in the same photostability chamber regulated at 25 °C.

Following the light exposure, all samples were buffer exchanged into formulation buffer, and were analyzed for biophysical, biochemical, and functional properties. No sample showed any change in physical appearance in terms of color or the presence of visible aggregates, except the light exposed sample containing tryptophan (Fig. 1C and D). The change in color in the tryptophan containing sample is due to the generation of N-formyl kynurenine, kynurenine, and other photodegradation products of the tryptophan (Li et al., 2014b).

3.2. Effect of photo-oxidation on the aggregation and hydrodynamic size of mAb8

Using reduced SDS-PAGE analysis, we first studied the changes in the monomer and aggregate content of mAb8 (Fig. 1E and F). In all samples, we observed two bands at ~25 and 50 kDa corresponding to the light chain (LC) and heavy chain (HC), respectively. However, in the case of light exposed mAb8 (lane 1 in Fig. 1E), we see two other bands at ~75 kDa and ~150 kDa, indicating mAb8 oligomerization. These two higher molecular weight bands were absent in the dark control (lane 2 in Fig. 1E). Since the SDS-PAGE was run under reducing conditions, these aggregates were not disulfide-linked. The presence of such covalent aggregates has been seen earlier in other light exposed antibodies, and the bands at ~75 kDa and ~150 kDa have been assigned to HC + LC and (HC + LC)$_2$ covalent aggregates (Cockrell et al.,

Table 1
Hydrodynamic radius of mAb8 samples determined using DLS.

Sample	Hydrodynamic radius (nm)	
	Light exposed	Dark Control
mAb8	5.8	5.6
mAb8 + Met	5.6	5.5
mAb8 + Trp	5.9	5.6
mAb8 + Arg	5.8	5.6
mAb8 + Sucrose	6.0	5.5
mAb8 + Trehalose	6.0	5.6

2015). Similar high molecular weight bands were also observed in light exposed mAb8 samples with different excipients, except in the case of methionine. The sample incubated with free methionine showed only one band at ~75 kDa, instead of two. None of the dark control samples showed any high molecular weight aggregation bands.

When samples were analyzed by dynamic light scattering (DLS) (Table 1 & Fig. 1B), we noted an increase in the hydrodynamic radius (R_H) for samples that were exposed to light compared to the respective dark controls except for the light exposed sample containing methionine. The light exposed mAb8 containing free methionine in solution has similar hydrodynamic radius as that of the dark control without methionine, indicating that methionine might be protecting mAb8 from photo-oxidation. This is consistent with the SDS-PAGE results (Fig. 1E and F) where less aggregates were observed for photo-exposed sample containing Met.

3.3. Effect of photo-oxidation on the structure of mAb8

Secondary and tertiary structure characterization was done on mAb8 to detect light-induced structural changes. We used far-UV CD to monitor the secondary structural changes of mAb8. The chromophore that absorbs in the far-UV range is the peptide group. mAbs being β-sheet proteins show a characteristic minima at 218 nm (Greenfield, 2006). As seen in Figs. 2A & 3A, no major changes were detected in the secondary structure of mAb8 upon exposing to light. To monitor the changes in tertiary structure, near-UV CD was used (Figs. 2B & 3B). Near-UV CD signal arises from the chiral environment of the side chains of aromatic residues tryptophan, tyrosine and phenylalanine in folded proteins. mAb8 did not show major changes upon photo degradation; however, the sample incubated with tryptophan (Fig. 2B, green) showed marked changes in the spectra. This change can be attributed to the excessive free radicals generated in this sample due to the degradation of free tryptophan present in solution. Changes in the environment around tryptophan residues can also be effectively probed using fluorescence spectroscopy (Lakowicz, 2006; Maity et al., 2012) (Figs. 2C & 3C). The fluorescence spectra of tryptophan containing sample (Fig. 2C, green) exposed to light showed a decrease in tryptophan fluorescence with a corresponding increase in the fluorescence at higher wavelengths, which is characteristic of photodegradation products of tryptophan that include kynurenine and N-formyl kynurenine (Kerwin and Remmele, 2007; Li et al., 2014b; Roy et al., 2009). All the dark controls with excipients or no excipients showed no changes in the fluorescence spectrum compared to that of the dark control mAb8.

3.4. Effect of photo-oxidation on the stability of mAb8

To identify changes in the thermodynamic stability of the protein, all samples were analyzed by differential scanning calorimetry (DSC). The DSC profile of mAb8 shows two unfolding events (Fig. 4A, yellow line). By comparing with the published DSC thermograms of similar IgG1 mAbs (Ionescu et al., 2008; Thiagarajan et al., 2016), the first peak in the DSC thermogram that occurs at lower temperature (with a T_m^1 of ~71 °C) can be attributed to the unfolding of the C_H2 domain,

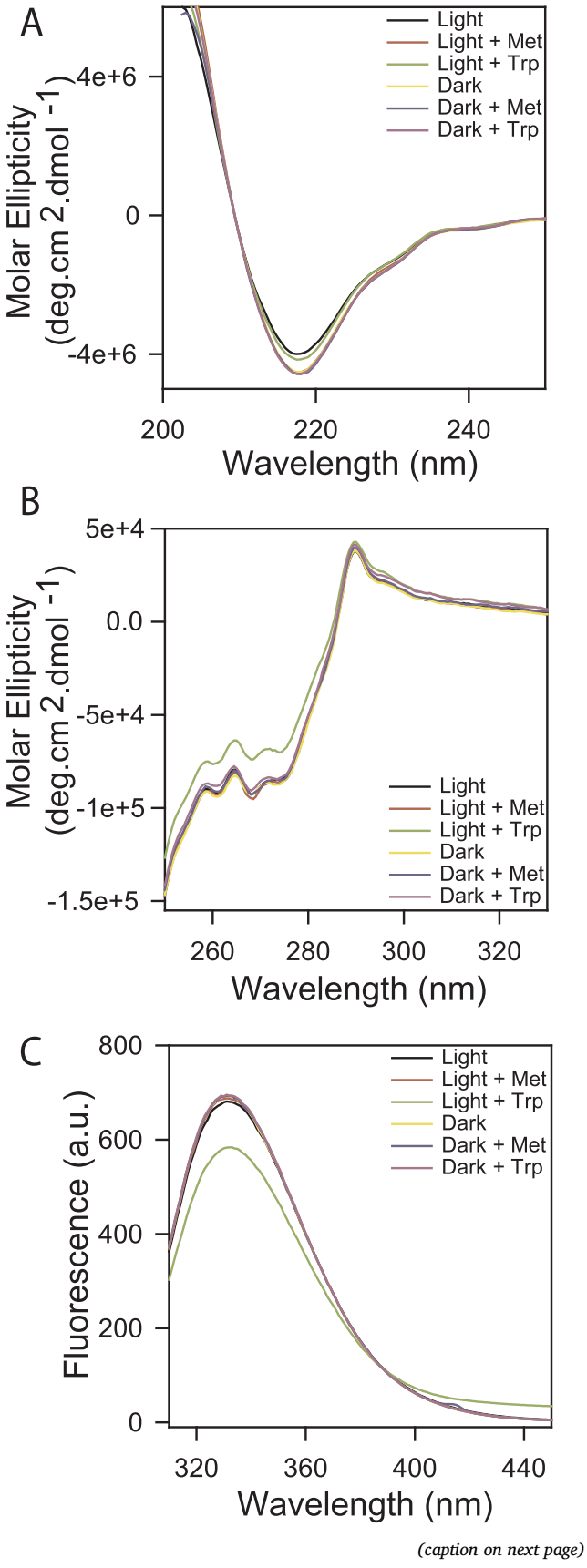

(caption on next page)

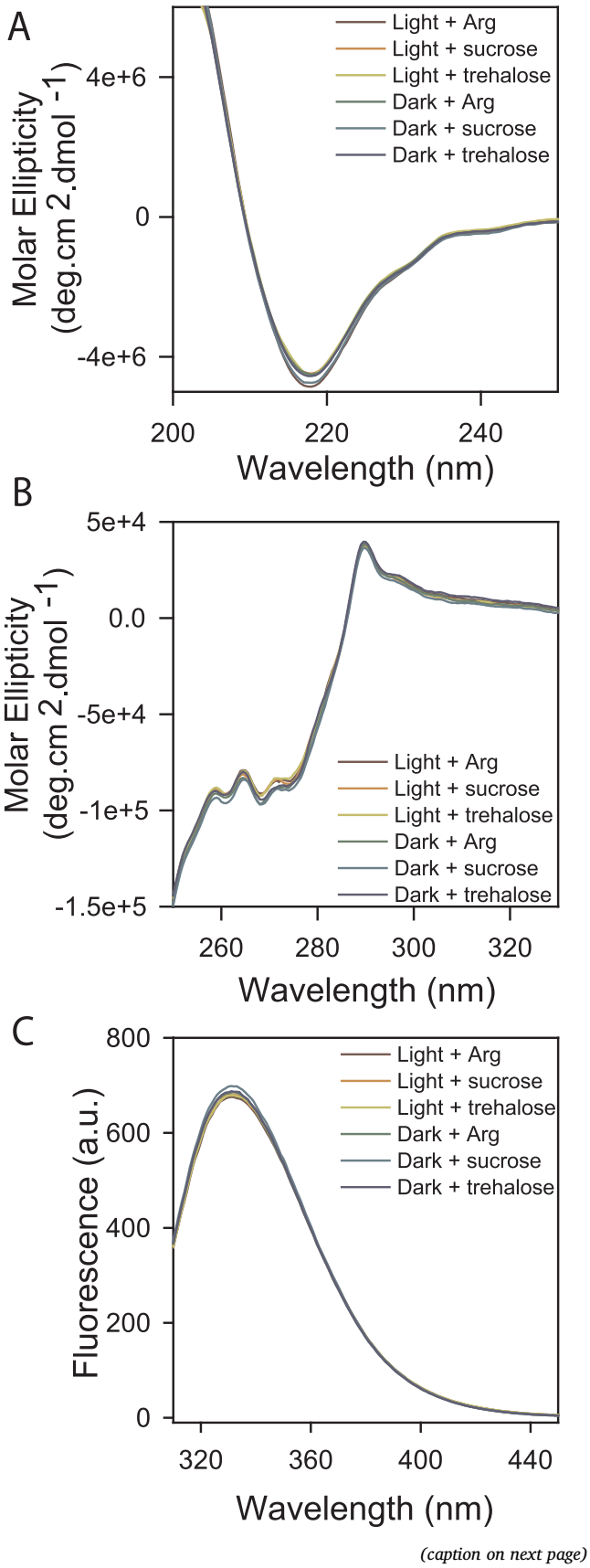

Fig. 2. Structural characterization of mAb8 samples. (A) Far-UV CD spectra of light exposed and corresponding dark control samples. (B) Near-UV CD spectra of light exposed and corresponding dark control samples. (C) Fluorescence spectra of light exposed and corresponding dark control samples. In all panels, black – mAb8 only (light), yellow – mAb8 only (dark), red – mAb8 with Met (light), magenta – mAb8 with Met (dark), green – mAb8 with Trp (light), blue – mAb8 with Trp (dark). (For interpretation of the references to colour in this figure legend, the reader is referred to the web version of this article.)

and the second larger peak occurring at higher temperatures (with a T_m^2 of ~82.5 °C) can be attributed to the unfolding of Fab and C_H3 domains. DSC thermograms indicated clear differences in the thermodynamic stability of light exposed mAb8 when compared to their corresponding dark control samples (Fig. 4A & B). Photo-oxidized mAb8 (Fig. 4A, black) showed destabilization of the C_H2 domain as indicated by unfolding of the first peak at lower temperatures compared to the dark control (Fig. 4A, yellow). Interestingly, the sample exposed to light in the presence of free methionine showed complete protection (Fig. 4A, red); the DSC thermogram closely matched with that of the dark control (Fig. 4A, yellow). The tryptophan containing sample (Fig. 4A, green) showed greater destabilization of the C_H2 domain compared to the light exposed sample without free tryptophan (Fig. 4A, black) because oxidation of free tryptophan present in solution is expected to produce more free radicals (Kerwin and Remmele, 2007; Roy et al., 2009). The presence of arginine, sucrose and trehalose did not seem to confer much protection to the protein and the results for these samples were similar to the mAb8 sample without excipients (Fig. 4B). This data shows that free methionine is effective in protecting mAb8 against photo-induced degradation under the excipient concentrations used in this study.

3.5. Effect of photo-oxidation on the aggregation of mAb8

Size exclusion chromatography was performed to monitor physical degradation (Table 2). Light exposed sample without any excipients showed loss of monomer along with the generation of aggregates (high molecular weight species; HMWS) and fragments (low molecular weight species; LMWS).

Of all the samples exposed to light that contained excipients, only the methionine containing sample had a similar level of monomer as dark controls (Table 2). This result shows that free methionine was able to exert its protective effect to such an extent that the mAb8 degradation was almost the same as storing the formulation in the dark.

3.6. Effect of photo-oxidation on the FcRn binding and function of mAb8

Measurements of biological activity of mAb8 were made on dark control and light-exposed sample without and with free L-methionine (Table 3). FcRn receptor binding assay was used to determine the effect of oxidation on the ability of mAb8 to bind to neonatal Fc receptor (FcRn). This activity is critical for the half-life of antibodies once they are administered to the patients (Gao et al., 2015; Liu et al., 2008; Roopenian and Akilesh, 2007). The FcRn receptor binding activity was partially lost in the case of photo-oxidized mAb8 (Table 3). For this binding, residues located in the C_H2 domain are crucial, and the decrease in FcRn binding was consistent with the DSC results that C_H2 domain was destabilized in the photo-oxidized mAb8 (Fig. 4A). Consistent with the DSC results, free methionine rescued the FcRn binding activity to significant extent (Table 3).

Antibody dependent cell-mediated cytotoxicity (ADCC) assay (Table 3) was performed on mAb8 to examine the effect of photo-oxidation on the correct functioning of both the Fab and Fc regions. Both Fc binding to FcγRs (Fc gamma receptors) and Fab binding to its target protein receptor are important for ADCC activity. mAb8 relies on two different types of functionalities. The first is target specific binding by

(caption on next page)

Fig. 3. Structural characterization of mAb8 samples. (A) Far-UV CD spectra of light exposed and corresponding dark control samples. (B) Near-UV CD spectra of light exposed and corresponding dark control samples. (C) Fluorescence spectra of light exposed and corresponding dark control samples. In all panels, maroon – mAb8 with Arg (light), dark green – mAb8 with Arg (dark), orange – mAb8 with sucrose (light), cyan – mAb8 with sucrose (dark), olive – mAb8 with trehalose (light), blue – mAb8 with trehalose (dark). (For interpretation of the references to colour in this figure legend, the reader is referred to the web version of this article.)

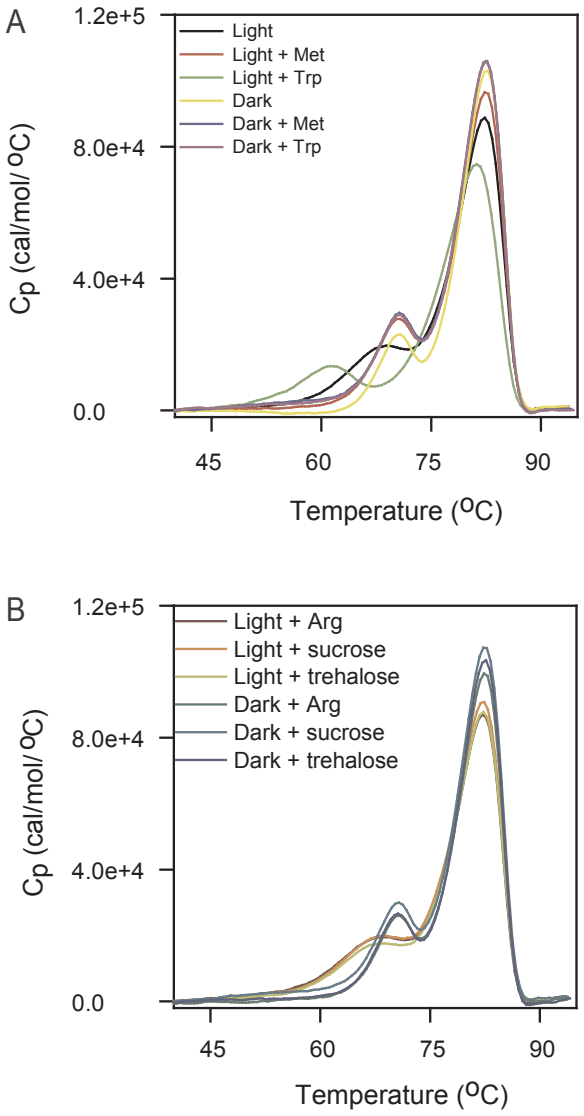

Fig. 4. Stability characterization of mAb8 samples. (A) Differential scanning calorimetry (DSC) thermograms of light exposed and corresponding dark control samples. Black – mAb8 only (light), yellow – mAb8 only (dark), red – mAb8 with Met (light), magenta – mAb8 with Met (dark), green – mAb8 with Trp (light), blue – mAb8 with Trp (dark). (B) DSC thermograms of light exposed and corresponding dark control samples. Maroon – mAb8 with Arg (light), dark green – mAb8 with Arg (dark), orange – mAb8 with sucrose (light), cyan – mAb8 with sucrose (dark), olive – mAb8 with trehalose (light), blue – mAb8 with trehalose (dark). (For interpretation of the references to colour in this figure legend, the reader is referred to the web version of this article.)

the Fab (antigen-binding fragment) domain and the second is immune-mediated effector functions – such as antibody dependent cell-mediated cytotoxicity (ADCC) which is regulated by both Fab and Fc regions. We observed decrease in the ADCC activity of photo-oxidized mAb8 compared to the dark control. In the presence of free methionine, this activity was affected to a lesser extent (Table 3).

We also performed the cell proliferation and target specific receptor binding assays (Table 3). Binding to the target specific receptor is important to the potency of mAb8. Loss in this activity leads to the loss of efficacy of the drug. Cell proliferation assay is a more comprehensive measure of the same activity; however, unlike the receptor binding assay, this is a cell-based assay and hence represents a more realistic assessment of the product efficacy. For the cell proliferation assay, the photo-oxidized sample again seems to be less effective, but free methionine rescued the activity completely (Table 3). Target receptor binding activity was not affected significantly by the photo-oxidation.

3.7. Identification of photo-oxidized residues in mAb8

To identify the residues that were oxidized by light, we subjected the samples to proteolysis-coupled mass spectrometry. Out of many peptides generated by trypsin proteolysis, only two peptides showed significant mass difference between dark mAb8 control and light exposed mAb8 forms. From the peptide sequence and the observed mass difference, two methionines Met252 and Met428 in the Fc region were identified to be oxidized (leading to a mass difference of 16 Daltons corresponding to the addition of an oxygen atom). In addition, the two Met residues were oxidized to different extents in the presence of different excipients. M252 was oxidized more than M428. In the absence of any excipients, M252 was oxidized about 41% and M428 was oxidized about 24%. Interestingly in the presence of free methionine, near-complete protection was observed, demonstrating the effectiveness of free Met to protect the protein from photo-oxidation (Table 4). The other three excipients, sucrose, trehalose and arginine did not protect the protein from photo-oxidation, under the excipient concentrations used here. Sample containing free tryptophan was the most affected due to the degradation of free tryptophan generating excess reactive oxygen species (ROS) that attacked the Met residues.

4. Discussion

Pharmaceutical proteins are susceptible to photodegradation. Exposure to light can come from ambient lighting in the manufacturing facility, during storage or transportation, and at the pharmacy or hospital before administration to the patient (Kerwin and Remmele, 2007; Rathore et al., 2010; Sreedhara et al., 2016). This light exposure in most cases is in the visible or near-UV wavelength region (Du et al., 2018; Nejadnik et al., 2018). Though proteins do not absorb in the visible spectrum, buffer components like polysorbates absorb in this region (Du et al., 2018). Current ICH guidelines recommend testing for photodegradation of protein drugs using specified light exposure protocols (Q1B, 1997). Photodegradation pathways characterized from light exposure can further help develop methods to prevent such degradation (Du et al., 2018; Hawe et al., 2012). The residues that are most sensitive to light exposure are those that absorb near-UV light, specifically tryptophan, tyrosine, phenylalanine and cysteine. Oxidation of these residues may further lead to secondary oxidation events of methionine and histidine (Kerwin and Remmele, 2007). Depending on the level of surface exposure, these residues may be oxidized to different levels (Liu et al., 2009; Sreedhara et al., 2013). Photodegradation can lead to structural changes (Kim et al., 2007; Liu et al., 2008; Sreedhara et al., 2016), chemical modification (Bane et al., 2017; Cleland et al., 1993; Kerwin and Remmele, 2007; Pattison et al., 2012; Roy et al., 2009), partial unfolding (Li et al., 2014b), destabilization (Liu et al., 2008; Mason et al., 2012), aggregation (Cockrell et al., 2015; Maity et al., 2009) and even loss of function in proteins (Wei et al., 2007). Additionally, generation of protein aggregates can lead to immunogenicity of therapeutic proteins, which is a major concern with protein drugs (Fradkin et al., 2014; Torosantucci et al., 2014).

In this study, we assessed photodegradation of a mAb from two aspects. The first was to understand the underlying mechanisms behind

Table 2
SEC quantification of aggregates (high molecular weight species; HMWS) and fragments (low molecular weight species; LMWS) in light-exposed mAb8 samples with respect to their dark controls.

Sample	% Monomer	% HMWS	% LMWS
Light exposed			
mAb8	87.2	9.4	3.5
mAb8 + Met	95.8	1.6	2.6
mAb8 + Trp	88.3	5.3	6.5
mAb8 + Arginine	87.5	8.1	4.4
mAb8 + Sucrose	88.2	8.1	3.8
mAb8 + Trehalose	86.7	9.0	4.4
Dark Controls			
mAb8	97.8	0.7	1.3
mAb8 + Met	97.9	0.8	1.2
mAb8 + Trp	97.9	0.8	1.2
mAb8 + Arginine	97.9	0.8	1.3
mAb8 + Sucrose	97.9	0.8	1.3
mAb8 + Trehalose	97.9	0.8	1.3

Table 3
Effect of photo-oxidation on mAb8 function. Experimental errors are within 10% of the measured values.

Sample Name	Assay Type			
	FcRn Binding Binding Activity (%)	ADCC Assay Relative ADCC Activity (%)	Cell Proliferation Assay Relative Potency (%)	Receptor Binding Binding Activity (%)
Reference Standard	98	–	–	100
mAb8 Fresh control	109	Used as assay control	103	100
mAb8 control	93	104	102	99
Light	52	72	79	91
Light + Met	84	84	103	90

the changes in structure, stability, aggregation, and function that occurred because of photo-oxidation on an antibody, and whether there exists any unifying mechanistic correlation between the changes in structure and stability with the aggregation and loss of antibody function. The second aspect was to identify the excipients that might protect the protein from light-induced oxidation and degradation. These excipients are frequently used in pharmaceutical formulations and have shown varying protection against light-induced damage to proteins (Grewal et al., 2014; Lam et al., 1997; Maity et al., 2009; Roy et al., 2009). Characterization with reducing SDS-PAGE gel showed that the photodegraded protein forms covalent aggregates whereas the dark control samples did not show these aggregates (Fig. 1E & F). Such formation of covalent aggregates has been seen in other antibodies upon photodegradation. These aggregates have been identified in earlier studies to form as a result of cross-linked HC-LC or HC-HC of two different antibody molecules (Cockrell et al., 2015). For all the excipients tested except Trp, we did not see major changes in the secondary and tertiary structure of mAb8. The sample exposed to light in the presence of free tryptophan did show browning of the solution (Fig. 1C), because tryptophan is a known photosensitizer and undergoes light-induced degradation to kynurenine, N-formyl kynurenine, and other degradation products. Consistently, the tertiary structural changes we see were only in the tryptophan containing sample (Fig. 2). In terms of thermodynamic stability, we noticed a change in the stability of the C_H2 domain of the protein when it was exposed to light in the presence of all tested excipients except methionine (Fig. 4). For the sample containing free methionine, the protein was completely protected from photodegradation. In terms of protein aggregation, all light exposed samples showed similar levels of aggregates (Table 2), and

Table 4
Photo-oxidized residues in mAb8 determined using proteolysis-coupled mass spectrometry.

Amino acid	Region	Dark Control						Light Exposed					
		mAb8	mAb8 + Met	mAb8 + Trp	mAb8 + Arg	mAb8 + Sucrose	mAb8 + Trehalose	mAb8	mAb8 + Met	mAb8 + Trp	mAb8 + Arg	mAb8 + Sucrose	mAb8 + Trehalose
M252	Fc-C_H2	4.5	4.2	4.9	4.4	4.4	4.4	40.5	5.9	98.3	47.2	46.8	49.3
M428	Fc-C_H3	1.0	0.9	1.2	1.0	1.1	1.1	23.8	1.9	98.6	27.6	27.2	27.7

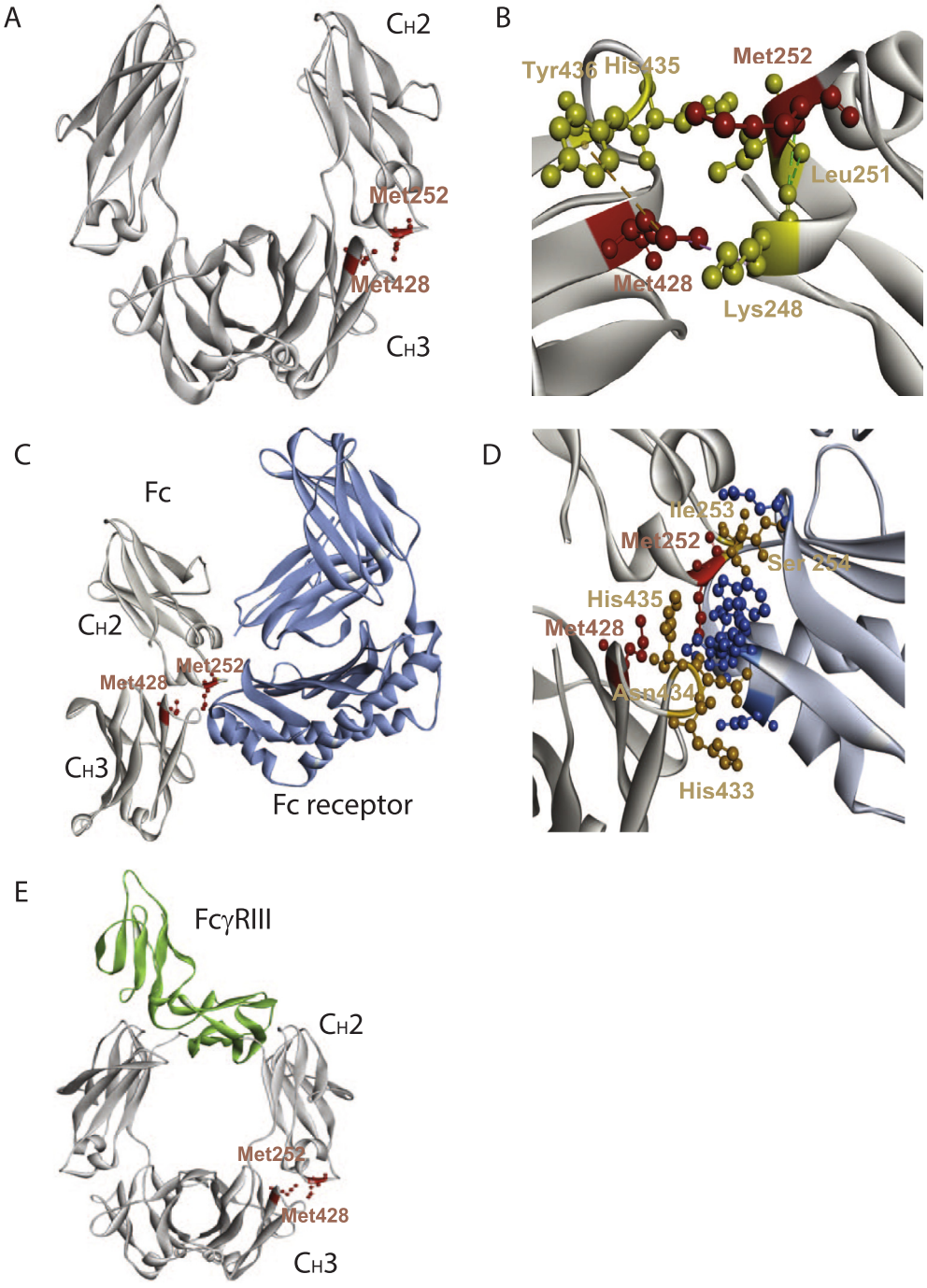

Fig. 5. Structural analysis of the effect of oxidation on mAb8. (A) Location of the two modified Met residues in the X-ray crystal structure of Fc (Protein Data Bank ID: 1FC1). Met252 is in the C_H2 domain, whereas Met428 is in the C_H3 domain. (B) Met252 and Met428 participate in the same hydrophobic network of interactions involving Lys248, Leu251, His435, and Tyr436. (C) X-ray crystal structure of Fc region bound to FcRn receptor (Protein Data Bank ID: 1FRT). Gray, blue, and red colors correspond to Fc, FcRn, and oxidized Met residues, respectively. Met252 and Met428 are in the binding interface between Fc and FcRn. (D) Various residues in the Fc region (yellow colored) surrounding the two chemically oxidized methionines Met252 and Met428 in Fc (red colored) form stabilizing interactions with the residues in the FcRn (blue colored). (E) X-ray crystal structure of Fc complex with FcγRIII receptor that controls ADCC activity. The two chemically oxidized residues Met252 and Met428 are far away from the binding interface. (For interpretation of the references to colour in this figure legend, the reader is referred to the web version of this article.)

again the protection from methionine was evident here in terms of the minimal loss of monomer and minimal generation of aggregates or degradants. These observations confirm the effectiveness of free methionine in protecting the mAb8 from light.

mAb8 contains 4 Met residues in each HC and 1 Met residue in each LC. Different Met residues can be susceptible to oxidation to different extents. The most vulnerable Met residues are typically located on the surface of protein and levels of oxidation have a direct correlation with the flexibility of local protein regions (Chu et al., 2004; Hui et al., 2015). Mass spectrometry analysis on light exposed mAb8 identified that two critical methionine residues M252 and M428 in Fc region were oxidized (Table 4). M252 and M428 are in the C_H2 and C_H3 domains, respectively (Fig. 5A). Although M428 is in the C_H3 domain, it participates in the same network of stabilizing interactions at the C_H2-C_H3 interface that include M252 (Fig. 5B). This explains why the C_H2 domain in the Fc region is destabilized upon exposure to light (Fig. 4A). In the presence of free methionine in solution, the Met 252 and Met 428 residues were completely protected in photo-exposed mAb8 (Table 4). More severe oxidation was observed in the tryptophan containing mAb8 sample, because of the generation of reactive oxygen species (ROS) by free tryptophan that may have led to almost complete oxidation of the two Met residues as seen in mass spectrometry data. This near-100% oxidation also resulted in significant changes in the tertiary structure of the protein as measured by near-UV CD (Fig. 2B & C). The other excipients, arginine, sucrose and trehalose were ineffective in protecting mAb8 from oxidation under the excipient concentrations used in this study. The efficacy of free methionine in protecting the protein is probably due to its sacrificial activity (Lam et al., 1997).

In functional assays (Table 3), a reduction in FcRn binding was observed for light-exposed mAb8. This is because the C_H2 domain determines binding to FcRn, and the same domain is destabilized upon light exposure (Fig. 4A). The two residues Met252 and Met428 that are oxidized are at the binding interface of Fc and FcRn (Fig. 5C). The other key residues involved in Fc receptor binding include Ile253, Ser254, His433, Asn434 and His435 (Shields et al., 2001), and all these residues are adjacent to the two oxidized Met residues Met252 and Met428 in the three-dimensional structure of Fc (Fig. 5D). Similar loss of FcRn binding has been observed in the past upon oxidation of Met252 and Met428 with oxidation of Met252 causing more serious loss of binding (Bertolotti-Ciarlet et al., 2009; Gao et al., 2015; Sokolowska et al., 2017). In the presence of free L-methionine, FcRn binding activity is much higher compared to light exposed mAb8 with no excipients, indicating the protection conferred by free methionine. In terms of ADCC activity, which depends on both Fab and Fc, none of the two oxidized residues Met252 and Met428 participate in the binding of Fc to FcγRs (Fig. 5E). This ADCC activity is partially retained in the free methionine containing sample (Table 3). Like ADCC activity, cell proliferation activity also decreased upon light exposure. However, this activity was completely protected when free methionine was present in the solution. Previously published studies show that FcRn binding in the Fc region can induce structural changes in the Fab region (Jensen et al., 2015). Similarly, changes in the complementarity-determining regions (CDR) have been shown to cause changes in the Fc region (Piche-Nicholas et al., 2018). Changes not just in the C_H2-C_H3 Fc region, but also C_H1, hinge flexibility, Fc-Fab elbow angle etc. can all play an important role in the structure of Fab region, thereby affecting its affinity and specificity (Yang et al., 2017). Further, these earlier studies indicate a cooperativity between the Fc and Fab regions of IgG1 where alterations in one region can affect the other (Yang et al., 2017). The loss of cooperativity between Fab and Fc because of the photo-oxidation of residues in Fc region might explain why the cell proliferation and ADCC activities, which are controlled by the Fab region in addition to Fc region, are affected in photo-oxidized mAb8. In contrast to cell proliferation, we did not see any changes in the Fab binding to its target receptor (Table 3), because this activity specifically depends on the Fab region, and no chemical modifications were observed in the Fab region (Table 4).

Alternative explanation for the loss of Fab activities can be the oxidation of tryptophans in CDRs of the variable domain (Bane et al., 2017; Mach et al., 1994). However, upon light exposure, we did not observe oxidation of any specific tryptophan residues in mAb8 when probed using mass spectrometry (Table 4). This is because tryptophan oxidation does not cause any mass difference unless the tryptophan is solvent exposed to molecular oxygen (Kerwin and Remmele, 2007). Although IgG1 antibodies typically contain 20–30 tryptophan residues, very few or none are vulnerable to irreversible photooxidation because of their relatively less solvent exposure (Grewal et al., 2014; Lam et al., 1997; Mach et al., 1994). mAb8 contains 22 tryptophans, and its structural analysis showed that these residues are buried in the protein interior making them inaccessible to the solvent. However, we did see some irreversible oxidation of tryptophan residues in mAb8 when free tryptophan was present in solution (Fig. 2C), which might have resulted in higher ROS generation as indicated by the browning of the solution. Tryptophans are known to be very efficient in transferring absorbed light energy to molecular triplet oxygen in solution and contribute to the generation of reactive oxygen species. Singlet oxygen and peroxide radicals are commonly generated in these cases; however, these species react rapidly with electron rich amino acids that include Trp (Li et al., 2014b; Sreedhara et al., 2013). N-formyl kynurenine and kynurenine are the major photodegradation products of tryptophan, which emit light at longer wavelengths above 350 nm compared to tryptophan (Roy et al., 2009). The fluorescence spectrum of light exposed mAb8 in the presence of free Trp did show a decrease in tryptophan fluorescence intensity at 332 nm with corresponding increase in the fluorescence at longer wavelengths (Fig. 2C), indicating the formation of N-formyl kynurenine and kynurenine. However, since we did not see any specific peptide which showed a clear mass difference upon oxidation that corresponds to tryptophan degradation, the oxidation observed in the case of light exposed mAb8 with free tryptophan must be non-specific. This minor oxidation did not change the local environment of the other unoxidized tryptophans, as evident from no change in the wavelength of the fluorescence emission maximum (332 nm) (Fig. 2C) or the absence of any near-UV CD spectral changes in the tryptophan region (> 292 nm) (Fig. 2B). In the wavelength region where tyrosines and phenyl alanines predominantly absorb (below 280 nm), near-UV CD showed a spectral change indicative of tertiary structural changes around these residues.

In the absence of free Trp in solution where we did not see either browning of the solution or the formation of N-formyl kyneurenin, autooxidation may significantly contribute to the oxidation of methionine residues in mAb8. Autooxidation is known to generate singlet oxygen, which is very efficient in converting Met to Met-sulfoxide (Schoneich, 2005, 2018). It might also be due to the degradation of excipients such as polysorbate 80 in the formulation which leads to the generation of ROS (Kerwin, 2008; Kishore et al., 2011a,b; Li et al., 2014a; Tomlinson et al., 2015). Photodegradation of proteins has been shown to be exacerbated in the presence of excipients such as polysorbates (Agarkhed et al., 2013). The levels and grade of excipients used in formulations can be an important factor in causing their oxidation and so should be chosen carefully (Singh et al., 2012). Hydrogen peroxide is the predominant oxidant degradation product of polysorbates, which attacks methionine residues (Jaeger et al., 1994; Ji et al., 2009). This could also explain why free methionine can be highly efficient in protecting proteins against oxidation, as it is a very efficient scavenger of singlet oxygen and peroxides.

We see a worsening of photooxidation in the presence of free Trp, and a similar phenomenon has been observed in the case of type I soluble tumor necrosis factor receptor (sTNFR1) (Roy et al., 2009). Interestingly, free Met could not protect the protein, which could be due to the lower levels of methionine used in the study (Roy et al., 2009). This is one reason why we tested whether higher concentration of methionine is efficient in protecting proteins from photo-oxidation. In the case of Trp as the excipient, Trp is a known photosensitizer and can generate a high concentration of reactive oxygen species (Li et al., 2014b), and correspondingly we observed increased mAb8 oxidation (Table 4). Free arginine was also unsuccessful in preventing aggregation of mAb8 under the excipient concentration we used. Arg prevents protein aggregation, by binding to the hydrophobic residues and by weak electrostatic interactions. However, these same weak electrostatic interactions may lead to charge shielding and reduce the colloidal stability of the protein (Sudrik et al., 2017). The disaccharides sucrose and trehalose were also unsuccessful in preventing the photo-oxidation of mAb8. Sucrose has been successfully used in the past to prevent oxidation of subtilisin (DePaz et al., 2000); however, it has been shown to be ineffective in protecting granulocyte-colony stimulating factor (Yin et al., 2005) and sTNFR1 (Roy et al., 2009), and in fact it increased the oxidation of rFVIIa (Soenderkaer et al., 2004). This increase was attributed to the presence of metal impurities in sucrose that may accentuate oxidation. However, it must be noted that fairly high concentrations (> 0.5 M) of these disaccharides are essential for the preferential exclusion-induced protective effects (DePaz et al., 2000; Kendrick et al., 1997; Lee and Timasheff, 1981; Timasheff, 2002). The lower concentrations used in this study may not have been sufficient. In the case of filled vials, photooxidation of protein formulations also depends significantly on the oxygen present in the vial headspace, and removing headspace oxygen by filling with nitrogen has been shown to prevent oxidation (Qi et al., 2009). Though we did not observe oxidation of histidine residues, light exposure can cause oxidation of histidine residues in some proteins, which are located near tryptophan residues (Bane et al., 2017). Such secondary oxidation due to

photosensitization by tryptophan can cause further degradation of pharmaceutical proteins. Therefore, it is very important to minimize exposure of therapeutic proteins to light. Use of primary and secondary package can considerably help protect the proteins from light. However light exposure is unavoidable in certain situations and it may have a detrimental effect on the protein. Assessing photosensitivity can help identify appropriate strategies to mitigate potential issues in protein formulation development.

5. Conclusion

In summary, our study identified the most photo-oxidation vulnerable residues in mAb8. Even though no structural differences were observed, we see a clear correlation between the loss of stability (DSC), generation of aggregates (HMWS), and loss of function. These effects can be explained based on the site of photo-oxidation, in particular, which residues are specifically oxidized, and their role in mAb8 structure, stability, and aggregation. Another interesting observation was the effectiveness of free methionine in providing protection from photo-induced degradation of mAb8. Together, these findings provided a comprehensive understanding of the unifying mechanism underlying the effect of photo-oxidation on the structure, stability, aggregation, and functional properties of mAb8.

Acknowledgements

This project was part of the PhD intern training program at Eli Lilly and Company under the supervision of Haripada Maity. We thank Eli Lilly and Company for providing mAb8 and all the other equipment and laboratory facilities utilized for this project. We also thank Babita Saxena Parekh for her support in the biological characterization assays and critical inputs in the project. We thank Michael R. De Felippis for reviewing the manuscript and providing valuable suggestions. We greatly appreciate the contribution of Shanmuuga Sundaram, Subarna Khan, Alice Matathia, Ping Carlson, and Hongli Li in biological characterization assays. We thank Ming-ching Hsieh for his support in LC-MS analysis. We thank David Bain, Brad Bendiak, John Carpenter and Lori Nield at the University of Colorado, for their valuable suggestions and feedback.

References

Agarkhed, M., O'Dell, C., Hsieh, M.C., Zhang, J., Goldstein, J., Srivastava, A., 2013. Effect of polysorbate 80 concentration on thermal and photostability of a monoclonal antibody. AAPS PharmSciTech 14, 1–9.

Arakawa, T., Ejima, D., Tsumoto, K., Obeyama, N., Tanaka, Y., Kita, Y., Timasheff, S.N., 2007a. Suppression of protein interactions by arginine: a proposed mechanism of the arginine effects. Biophys. Chem. 127, 1–8.

Arakawa, T., Tsumoto, K., Kita, Y., Chang, B., Ejima, D., 2007b. Biotechnology applications of amino acids in protein purification and formulations. Amino Acids 33, 587–605.

Bane, J., Mozziconacci, O., Yi, L., Wang, Y.J., Sreedhara, A., Schoneich, C., 2017. Photo-oxidation of IgG1 and model peptides: detection and analysis of triply oxidized his and trp side chain cleavage products. Pharm. Res. 34, 229–242.

Bertolotti-Ciarlet, A., Wang, W., Lownes, R., Pristatsky, P., Fang, Y., McKelvey, T., Li, Y., Li, Y., Drummond, J., Prueksaritanont, T., Vlasak, J., 2009. Impact of methionine oxidation on the binding of human IgG1 to Fc Rn and Fc gamma receptors. Mol. Immunol. 46, 1878–1882.

Bommana, R., Chai, Q., Schoneich, C., Weiss 4th, W.F., Majumdar, R., 2018. Understanding the increased aggregation propensity of a light-exposed IgG1 monoclonal antibody using hydrogen exchange mass spectrometry, biophysical characterization, and structural analysis. J. Pharm. Sci. 107, 1498–1511.

Bruner, M.W., Goldstein, J., Middaugh, C.R., Brooks, M.A., Volkin, D.B., 1997. Size exclusion HPLC method for the determination of acidic fibroblast growth factor in viscous formulations. J. Pharm. Biomed. Anal. 15, 1929–1935.

Chi, E.Y., Krishnan, S., Randolph, T.W., Carpenter, J.F., 2003. Physical stability of proteins in aqueous solution: mechanism and driving forces in nonnative protein aggregation. Pharm. Res. 20, 1325–1336.

Chu, J.W., Yin, J., Brooks, B.R., Wang, D.I., Ricci, M.S., Brems, D.N., Trout, B.L., 2004. A comprehensive picture of non-site specific oxidation of methionine residues by peroxides in protein pharmaceuticals. J. Pharm. Sci. 93, 3096–3102.

Cipriano, D., Burnham, M., Hughes, J.V., 2012. Effectiveness of various processing steps for viral clearance of therapeutic proteins: database analyses of commonly used steps. Methods Mol. Biol. 899, 277–292.

Cleland, J.L., Powell, M.F., Shire, S.J., 1993. The development of stable protein formulations: a close look at protein aggregation, deamidation, and oxidation. Crit. Rev. Ther. Drug Carrier Syst. 10, 307–377.

Cockrell, G.M., Wolfe, M.S., Wolfe, J.L., Schoneich, C., 2015. Photoinduced aggregation of a model antibody-drug conjugate. Mol. Pharm. 12, 1784–1797.

DePaz, R.A., Barnett, C.C., Dale, D.A., Carpenter, J.F., Gaertner, A.L., Randolph, T.W., 2000. The excluding effects of sucrose on a protein chemical degradation pathway: methionine oxidation in subtilisin. Arch. Biochem. Biophys. 384, 123–132.

Du, C., Barnett, G., Borwankar, A., Lewandowski, A., Singh, N., Ghose, S., Borys, M., Li, Z.J., 2018. Protection of therapeutic antibodies from visible light induced degradation: use safe light in manufacturing and storage. Eur. J. Pharm. Biopharm. 127, 37–43.

FDA, 2017. Purple book: Lists of Licensed Biological Products with Reference Product Exclusivity and Biosimilarity or Interchangeability Evaluations.

Fradkin, A.H., Mozziconacci, O., Schoneich, C., Carpenter, J.F., Randolph, T.W., 2014. UV photodegradation of murine growth hormone: chemical analysis and immunogenicity consequences. Eur. J. Pharm. Biopharm. 87, 395–402.

Gao, X., Ji, J.A., Veeravalli, K., Wang, Y.J., Zhang, T., McGreevy, W., Zheng, K., Kelley, R.F., Laird, M.W., Liu, J., Cromwell, M., 2015. Effect of individual Fc methionine oxidation on FcRn binding: Met252 oxidation impairs FcRn binding more profoundly than Met428 oxidation. J. Pharm. Sci. 104, 368–377.

Greenfield, N.J., 2006. Using circular dichroism spectra to estimate protein secondary structure. Nat. Protoc. 1, 2876–2890.

Grewal, P., Mallaney, M., Lau, K., Sreedhara, A., 2014. Screening methods to identify indole derivatives that protect against reactive oxygen species induced tryptophan oxidation in proteins. Mol. Pharm. 11, 1259–1272.

Ha, E., Wang, W., Wang, Y.J., 2002. Peroxide formation in polysorbate 80 and protein stability. J. Pharm. Sci. 91, 2252–2264.

Hawe, A., Wiggenhorn, M., van de Weert, M., Garbe, J.H., Mahler, H.C., Jiskoot, W., 2012. Forced degradation of therapeutic proteins. J. Pharm. Sci. 101, 895–913.

Hui, A., Lam, X.M., Kuehl, C., Grauschopf, U., Wang, Y.J., 2015. Kinetic modeling of methionine oxidation in monoclonal antibodies from hydrogen peroxide spiking studies. PDA J. Pharm. Sci. Technol. 69, 511–525.

Ionescu, R.M., Vlasak, J., Price, C., Kirchmeier, M., 2008. Contribution of variable domains to the stability of humanized IgG1 monoclonal antibodies. J. Pharm. Sci. 97, 1414–1426.

Jaeger, J., Sorensen, K., Wolff, S.P., 1994. Peroxide accumulation in detergents. J. Biochem. Biophys. Methods 29, 77–81.

Jensen, P.F., Larraillet, V., Schlothauer, T., Kettenberger, H., Hilger, M., Rand, K.D., 2015. Investigating the interaction between the neonatal Fc receptor and monoclonal antibody variants by hydrogen/deuterium exchange mass spectrometry. Mol. Cell Proteomics 14, 148–161.

Ji, J.A., Zhang, B., Cheng, W., Wang, Y.J., 2009. Methionine, tryptophan, and histidine oxidation in a model protein, PTH: mechanisms and stabilization. J. Pharm. Sci. 98, 4485–4500.

Kendrick, B.S., Chang, B.S., Arakawa, T., Peterson, B., Randolph, T.W., Manning, M.C., Carpenter, J.F., 1997. Preferential exclusion of sucrose from recombinant interleukin-1 receptor antagonist: role in restricted conformational mobility and compaction of native state. Proc. Natl. Acad. Sci. U.S.A. 94, 11917–11922.

Kerwin, B.A., 2008. Polysorbates 20 and 80 used in the formulation of protein biotherapeutics: structure and degradation pathways. J. Pharm. Sci. 97, 2924–2935.

Kerwin, B.A., Remmele Jr., R.L., 2007. Protect from light: photodegradation and protein biologics. J. Pharm. Sci. 96, 1468–1479.

Kim, H.H., Lee, Y.M., Suh, J.K., Song, N.W., 2007. Photodegradation mechanism and reaction kinetics of recombinant human interferon-alpha2a. Photochem. Photobiol. Sci. 6, 171–180.

Kishore, R.S., Kiese, S., Fischer, S., Pappenberger, A., Grauschopf, U., Mahler, H.C., 2011a. The degradation of polysorbates 20 and 80 and its potential impact on the stability of biotherapeutics. Pharm. Res. 28, 1194–1210.

Kishore, R.S., Pappenberger, A., Dauphin, I.B., Ross, A., Buergi, B., Staempfli, A., Mahler, H.C., 2011b. Degradation of polysorbates 20 and 80: studies on thermal autoxidation and hydrolysis. J. Pharm. Sci. 100, 721–731.

Knepp, V.M., Whatley, J.L., Muchnik, A., Calderwood, T.S., 1996. Identification of antioxidants for prevention of peroxide-mediated oxidation of recombinant human ciliary neurotrophic factor and recombinant human nerve growth factor. PDA J. Pharm. Sci. Technol. 50, 163–171.

Lagasse, H.A., Alexaki, A., Simhadri, V.L., Katagiri, N.H., Jankowski, W., Sauna, Z.E., Kimchi-Sarfaty, C., 2017. Recent Advances in (Therapeutic Protein) Drug Development. F1000Res 6, 113.

Lakowicz, J.R., 2006. Principles of Fluorescence Spectroscopy, third ed. Springer Science, New York.

Lam, X.M., Yang, J.Y., Cleland, J.L., 1997. Antioxidants for prevention of methionine oxidation in recombinant monoclonal antibody HER2. J. Pharm. Sci. 86, 1250–1255.

Lee, J.C., Timasheff, S.N., 1981. The stabilization of proteins by sucrose. J. Biol. Chem. 256, 7193–7201.

Li, S., Schoneich, C., Borchardt, R.T., 1995. Chemical instability of protein pharmaceuticals: mechanisms of oxidation and strategies for stabilization. Biotechnol. Bioeng. 48, 490–500.

Li, Y., Hewitt, D., Lentz, Y.K., Ji, J.A., Zhang, T.Y., Zhang, K., 2014a. Characterization and stability study of polysorbate 20 in therapeutic monoclonal antibody formulation by multidimensional ultrahigh-performance liquid chromatography-charged aerosol detection-mass spectrometry. Anal. Chem. 86, 5150–5157.

Li, Y., Polozova, A., Gruia, F., Feng, J., 2014b. Characterization of the degradation products of a color-changed monoclonal antibody: tryptophan-derived chromophores. Anal. Chem. 86, 6850–6857.

Liu, D., Ren, D., Huang, H., Dankberg, J., Rosenfeld, R., Cocco, M.J., Li, L., Brems, D.N., Remmele Jr., R.L., 2008. Structure and stability changes of human IgG1 Fc as a consequence of methionine oxidation. Biochemistry 47, 5088–5100.
Liu, H., Gaza-Bulseco, G., Zhou, L., 2009. Mass spectrometry analysis of photo-induced methionine oxidation of a recombinant human monoclonal antibody. J. Am. Soc. Mass Spectrom. 20, 525–528.
Lorenz, C.M., Wolk, B.M., Quan, C.P., Alcala, E.W., Eng, M., McDonald, D.J., Matthews, T.C., 2009. The effect of low intensity ultraviolet-c light on monoclonal antibodies. Biotechnol. Prog. 25, 476–482.
Mach, H., Burke, C.J., Sanyal, G., Tsai, P.-K., Volkin, D.B., Middaugh, C.R., 1994. Origin of the photosensitivity of a monoclonal immunoglobulin G, Formulation and delivery of proteins and peptides. ACS Symp. Series 567, 72–84.
Maity, H., Lai, Y., Srivastava, A., Goldstein, J., 2012. Principles and applications of selective biophysical methods for characterization and comparability assessment of a monoclonal antibody. Curr. Pharm. Biotechnol. 13, 2078–2101.
Maity, H., O'Dell, C., Srivastava, A., Goldstein, J., 2009. Effects of arginine on photostability and thermal stability of IgG1 monoclonal antibodies. Curr. Pharm. Biotechnol. 10, 761–766.
Mason, B.D., Schoneich, C., Kerwin, B.A., 2012. Effect of pH and light on aggregation and conformation of an IgG1 mAb. Mol. Pharm. 9, 774–790.
Miller, B.L., Hageman, M.J., Thamann, T.J., Barron, L.B., Schoneich, C., 2003. Solid-state photodegradation of bovine somatotropin (bovine growth hormone): evidence for tryptophan-mediated photooxidation of disulfide bonds. J. Pharm. Sci. 92, 1698–1709.
Nejadnik, M.R., Randolph, T.W., Volkin, D.B., Schoneich, C., Carpenter, J.F., Crommelin, D.J.A., Jiskoot, W., 2018. Postproduction handling and administration of protein pharmaceuticals and potential instability issues. J. Pharm. Sci. http://dx.doi.org/10.1016/j.xphs.2018.04.005.
Nowak, C., Cheung, J.K., Dellatore, S.M., Katiyar, A., Bhat, R., Sun, J., Ponniah, G., Neill, A., Mason, B., Beck, A., Liu, H., 2017. Forced degradation of recombinant monoclonal antibodies: a practical guide. mAbs 9, 1217–1230.
Pattison, D.I., Rahmanto, A.S., Davies, M.J., 2012. Photo-oxidation of proteins. Photochem. Photobiol. Sci. 11, 38–53.
Piche-Nicholas, N.M., Avery, L.B., King, A.C., Kavosi, M., Wang, M., O'Hara, D.M., Tchistiakova, L., Katragadda, M., 2018. Changes in complementarity-determining regions significantly alter IgG binding to the neonatal Fc receptor (FcRn) and pharmacokinetics. mAbs 10, 81–94.
Q1B, 1997. Stability testing: Photostability Testing of New Drug Substances and Products. Federal Registry 27115–27122.
Qi, P., Volkin, D.B., Zhao, H., Nedved, M.L., Hughes, R., Bass, R., Yi, S.C., Panek, M.E., Wang, D., Dalmonte, P., Bond, M.D., 2009. Characterization of the photodegradation of a human IgG1 monoclonal antibody formulated as a high-concentration liquid dosage form. J. Pharm. Sci. 98, 3117–3130.
Rathore, N., Rajan, R.S., Freund, E., 2010. Impact of manufacturing processes on drug product stability and quality. Formulation and process development strategies for manufacturing biopharmaceuticals. John Wiley & Sons, Inc., pp. 917–940.
Roopenian, D.C., Akilesh, S., 2007. FcRn: the neonatal Fc receptor comes of age. Nat. Rev. Immunol. 7, 715–725.
Roy, S., Mason, B.D., Schoneich, C.S., Carpenter, J.F., Boone, T.C., Kerwin, B.A., 2009. Light-induced aggregation of type I soluble tumor necrosis factor receptor. J. Pharm. Sci. 98, 3182–3199.
Schoneich, C., 2005. Methionine oxidation by reactive oxygen species: reaction mechanisms and relevance to Alzheimer's disease. Biochim. Biophys. Acta 1703, 111–119.
Schoneich, C., 2018. Novel chemical degradation pathways of proteins mediated by tryptophan oxidation: tryptophan side chain fragmentation. J. Pharm. Pharmacol. 70, 655–665.
Shields, R.L., Namenuk, A.K., Hong, K., Meng, Y.G., Rae, J., Briggs, J., Xie, D., Lai, J., Stadlen, A., Li, B., Fox, J.A., Presta, L.G., 2001. High resolution mapping of the binding site on human IgG1 for Fc gamma RI, Fc gamma RII, Fc gamma RIII, and FcRn and design of IgG1 variants with improved binding to the Fc gamma R. J. Biol. Chem. 276, 6591–6604.
Singh, S.R., Zhang, J., O'Dell, C., Hsieh, M.C., Goldstein, J., Liu, J., Srivastava, A., 2012. Effect of polysorbate 80 quality on photostability of a monoclonal antibody. AAPS PharmSciTech 13, 422–430.
Soenderkaer, S., Carpenter, J.F., van de Weert, M., Hansen, L.L., Flink, J., Frokjaer, S., 2004. Effects of sucrose on rFVIIa aggregation and methionine oxidation. Eur. J. Pharm. Sci. 21, 597–606.
Sokolowska, I., Mo, J., Dong, J., Lewis, M.J., Hu, P., 2017. Subunit mass analysis for monitoring antibody oxidation. mAbs-Austin 9, 498–505.
Sreedhara, A., Lau, K., Li, C., Hosken, B., Macchi, F., Zhan, D., Shen, A., Steinmann, D., Schoneich, C., Lentz, Y., 2013. Role of surface exposed tryptophan as substrate generators for the antibody catalyzed water oxidation pathway. Mol. Pharm. 10, 278–288.
Sreedhara, A., Yin, J., Joyce, M., Lau, K., Wecksler, A.T., Deperalta, G., Yi, L., John Wang, Y., Kabakoff, B., Kishore, R.S., 2016. Effect of ambient light on IgG1 monoclonal antibodies during drug product processing and development. Eur. J. Pharm. Biopharm. 100, 38–46.
Sudrik, C., Cloutier, T., Pham, P., Samra, H.S., Trout, B.L., 2017. Preferential interactions of trehalose, L-arginine.HCl and sodium chloride with therapeutically relevant IgG1 monoclonal antibodies. mAbs 9, 1155–1168.
Thiagarajan, G., Semple, A., James, J.K., Cheung, J.K., Shameem, M., 2016. A comparison of biophysical characterization techniques in predicting monoclonal antibody stability. mAbs 8, 1088–1097.
Timasheff, S.N., 2002. Protein-solvent preferential interactions, protein hydration, and the modulation of biochemical reactions by solvent components. Proc. Natl. Acad. Sci. U.S.A. 99, 9721–9726.
Tomlinson, A., Demeule, B., Lin, B., Yadav, S., 2015. Polysorbate 20 degradation in biopharmaceutical formulations: quantification of free fatty acids, characterization of particulates, and insights into the degradation mechanism. Mol. Pharm. 12, 3805–3815.
Torosantucci, R., Schoneich, C., Jiskoot, W., 2014. Oxidation of therapeutic proteins and peptides: structural and biological consequences. Pharm. Res. 31, 541–553.
Wei, Z., Feng, J., Lin, H.Y., Mullapudi, S., Bishop, E., Tous, G.I., Casas-Finet, J., Hakki, F., Strouse, R., Schenerman, M.A., 2007. Identification of a single tryptophan residue as critical for binding activity in a humanized monoclonal antibody against respiratory syncytial virus. Anal. Chem. 79, 2797–2805.
Yang, D., Kroe-Barrett, R., Singh, S., Roberts, C.J., Laue, T.M., 2017. IgG cooperativity – is there allostery? implications for antibody functions and therapeutic antibody development. mAbs 9, 1231–1252.
Yin, J., Chu, J.W., Ricci, M.S., Brems, D.N., Wang, D.I., Trout, B.L., 2005. Effects of excipients on the hydrogen peroxide-induced oxidation of methionine residues in granulocyte colony-stimulating factor. Pharm. Res. 22, 141–147.
Zbacnik, T.J., Holcomb, R.E., Katayama, D.S., Murphy, B.M., Payne, R.W., Coccaro, R.C., Evans, G.J., Matsuura, J.E., Henry, C.S., Manning, M.C., 2017. Role of buffers in protein formulations. J. Pharm. Sci. 106, 713–733.